Int J Clin Exp Med 2018;11(7):7192-7199
www.ijcem.com /ISSN:1940-5901/IJCEM0061212

Original Article

Liver protein spectrum in a rat liver injury model

Huan Wang[1*], Shan Tong[2*], Hongmei Han[3], Tuul Khalzaabaast[4], Bagenna Bao[1]

[1]School of Mongolian Medicine and Pharmaceutical Sciences, [4]College of Mongolian Medicine, Inner Mongolia University for The Nationalities, Tongliao, Inner Mongolia, P. R. China; [2]Mongolian Medicine Surgery, [3]Mongolian Medicine Digestive Internal Medicine, Affiliated Hospital of Inner Mongolia University for The Nationalities, Tongliao, Inner Mongolia, P. R. China. [*]Co-first authors.

Received May 15, 2017; Accepted December 13, 2017; Epub July 15, 2018; Published July 30, 2018

Abstract: This study aimed to identify the potential key proteins associated with liver injury based on the established rat model. The rat liver injury model was established using the method of pyloric ligation and then was confirmed by determination of serum enzymes and bilirubins as well as liver glutathione peroxidase and liver index. The protein spectrum of liver samples was analyzed using high performance liquid chromatography-mass spectrometry system. Subsequently, the differentially expressed proteins (DEPs) between the model rats and controls were identified, and their potential functions and interactions were further analyzed. The rat liver injury model was successfully established. According to the analysis of liver protein spectrum, a total of 147 DEPs were identified, including 80 upregulated and 67 downregulated DEPs in the model group. In the PPI network, upregulated *Stat3* which had the highest degree interacted with multiple upregulated proteins, such as *Junb*, *Fgg*, and *Hmox1*, as well as downregulated proteins like *Serpina3c* and *Tgfb1i1*. Furthermore, *Stat3* and *Hmox1* were predicted to be associated with immunity. The DEPs may play crucial roles in the liver injury. These results are expected to contribute to the diagnosis and therapy of liver injury.

Keywords: Differentially expressed protein, liver injury, model, network, protein spectrum

Introduction

Idiosyncratic drug-induced liver injury (DILI) is a common event because of the expanding use of prescription drugs, accounting for about 13% of acute liver failure cases in the United States [1]. It is the most frequent adverse drug reaction (ADR) that leads to termination of development programs for new drugs, failure of approval by supervision agencies, even withdrawal of licensed drugs [2]. Despite the great effect of DILI on both development of important new medications and patient health, the risk factors and mechanisms of idiosyncratic ADRs that lead to liver injury are still little understood.

In the past few years, a set of proteins and biological functions have been found to be associated with DILI. For example, a mass spectrometry (MS)-based quantitative proteomic approach has identified 92 differentially expressed priority 1 proteins between the DILI patients and controls [3]. This study has also discovered that apolipoprotein E expression is able to differentiate DILI patients from the controls [3]. Deficiency of transmembrane thioredoxin-related protein can cause increased sensitivity to the toxicants and developed severe liver damage [4]. Furthermore, activator protein 1 (AP-1) proteins, such as Jun and Fos, have also been reported to be implicated in the development of liver injury [5]. Additionally, a recent study has reported that the phosphorylation of CCAAT/Enhancer Binding Protein-β (C/EBPβ)-Thr217 is essential for the activation of the inflammasome in liver macrophages and liver injury [6]. However, numerous proteins and protein-protein interactions (PPIs) that are related to liver injury have still not been detected.

In this study, pyloric ligation was used to induce rat liver injury, and high performance liquid chromatography-MS (HPLC-MS) system was utilized to scan the liver protein spectrum in rat liver injury models and controls. Expression difference of proteins was analyzed, and the potential functions and interactions of the differentially expressed proteins (DEPs) were further investigated. These results were expected to be helpful for a better understanding of the pathogenesis of liver injury, and provide potential biomarkers for the diagnosis and therapy of liver injury.

Table 1. The expression levels of serum enzymes and bilirubins in rat liver injury models and controls

Group	Number of animals	AST ($U \cdot L^{-1}$)	ALT ($U \cdot L^{-1}$)	ALP ($U \cdot L^{-1}$)	BILD2 ($U \cdot L^{-1}$)	BILD3 ($U \cdot L^{-1}$)
Model	10	861.63±195.63**	198.25±60.05**	143.67±26.53*	0.8417±0.1605**	0.8917±0.3303**
Control	10	149.58±28.52	30.43±4.72	121.92±22.01	0.5833±0.1624	0.3750±0.2586

AST, aspartate aminotransferase; ALT, alanine aminotransferase; ALP, serum alkaline phosphatase; BILD2, serum direct bilirubin; BILT3, serum total bilirubin. *P < 0.05; **P < 0.01.

Table 2. The expression of glutathione peroxidase in liver and liver index in rat liver injury models and controls

Group	Number of animals	GSH-PX ($U \cdot L^{-1}$)	Liver index (%)
Model	10	210.76±45.55*	2.88±0.15*
Control	10	259.12±55.22	2.67±0.17

GSH-PX, glutathione peroxidase. *, P < 0.05.

Materials and methods

Animals and grouping

A total of 20 specific-pathogen-free Wistar male rats (180-220 g) were purchased from Changchun Yisi experimental animal technology co., LTD (certification number: SCXK (JI)-2011-0004, Changchun, China). According to the random number table, all of rats were divided into five groups randomly: the model group, and control group. Each group included 10 rats. All of rats were fed under pathogen-free conditions and underwent a reversed 12:12 h light/dark cycle. The room temperature was kept constant at 22-25°C, and the relative humidity at 50%. After two days of adaptation, all of rats underwent fasting but not water deprivation for 24 h. Subsequently, the animals were narcotized by 10% chloral hydrate. For animals in the model group, they received pyloric ligation, and then underwent fasting but not water deprivation for 18 h. These animals were fed separately. Animals in the control group did not undergo any surgery. Afterwards, they were narcotized by 10% chloral hydrate, and blood was sampled from abdominal aorta. The liver was also sampled, washed and weighed. Part of the liver sample was immediately quick-frozen in liquid nitrogen and then stored at -80°C.

Determination of blood and liver indexes

Serum aminotransferase levels [aspartate aminotransferase (AST) and alanine aminotransferase (ALT)], serum direct bilirubin (BILD2), and serum total bilirubin (BILT3) were measured using the Roche test kits. The levels of serum alkaline phosphatase (ALP) were determined using an alkaline phosphatase kit (Roche Molecular Biochemicals). Furthermore, the activity of glutathione peroxidase (GSH-PX) in the liver was determined using the test kit obtained from the Nanjing Jiancheng biological engineering center (Nanjing, China). Additionally, following a liver index was calculated as liver mass/rat mass × 100%.

Tandem mass tag (TMT)-labeled protein spectrum

Proteins in the liver samples were extracted using the radio immunoprecipitation assay buffer method. After the quantitative determination by BCA Protein Assay Kit (Pierce), 100 μg protein in each sample was used for the TMT labeling, which was conducted according to the instructions of the TMT isobaric Mass Tagging Kits and Reagents (Pierce). Subsequently, the TMT-labeled protein samples underwent vacuum concentration, and then were dissolved. The labeled protein solution (pH 10) was centrifuged and the supernatant was graded in the C18 column using a gradient elution pattern. The 2% acetonitrile mixed with 98% H_2O (pH 10) was used as A phase, and 90% acetonitrile mixed with 10% H_2O (pH 10) was used as B phase. Flow rate was set as 1 mL/min.

After the gradient elution, samples were input into the Q Exactive high performance liquid chromatography (LC) system (Thermo Fisher Scientific, Hudson, NH, USA) equipped with NCS3500 MS system (scan range: m/z 350-1600, Dionex, Sunnyvale, CA, USA). The 0.1% formic acid mixed with 99.9% H_2O was used as A phase in LC, and 99.9% acetonitrile mixed with 0.1% formic acid was used as B phase in LC. Flow rate was set as 300 nL/min.

Data preprocessing and Identification of DEPs

The proteome database (human-refseq-20140-303-71465s.fasta) downloaded from National

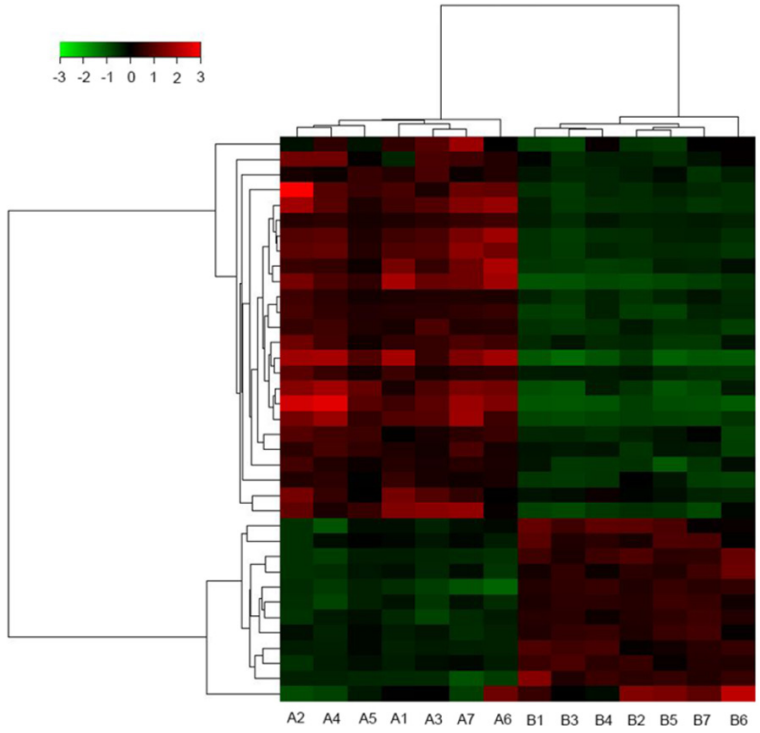

Figure 1. The clustering heat map displaying the differentially expressed proteins in the rat liver injury models and the controls. A1-A7 represent the liver samples from rat liver injury models, and B1-B7 represent the liver samples from control rats. The red diamonds represent the upregulated proteins, and the green diamonds represent the downregulated proteins.

Center of Biotechnology Information (NCBI) was used for the analysis of the generated protein spectrum data by the Proteome Discoverer software. The relatively credible data of polypeptides and proteins were retained. Afterwards, the DEPs between the model and control groups were identified based on the expression data of polypeptides and proteins. The cut-off criteria were set as false discovery rate (FDR) < 0.05 and fold change (FC) > 1.5.

Functional enrichment analyses of DEPs

Gene Ontology (GO) enrichment analysis and Kyoto Encyclopedia of Genes and Genomes (KEGG) pathway analysis were carried out using KOBAS (KEGG Orthology Based Annotation System, http://web.ttsnetwork.net/KS/pages/indeX.jsp) [7]. *P*-value < 0.05 was set as the threshold.

Construction of protein-protein interaction (PPI) network

For all of the identified DEPs, PPI network was constructed with information from a well-known online server, Search Tool for the Retrieval of Interacting Genes/Proteins version 10 (STRING v10) [8]. Only the PPIs with confidence score > 0.4 were defined as significant PPIs, which were utilized to construct the PPI network. Network was visualized using software Cytoscape version 2.8 [9]. In the network, node represents a protein; line represents the interaction between two proteins; and the degree of a node is equal to the number of nodes interacting with this node.

Statistical analysis

Data were presented as mean ± standard deviation from three separate experiments performed in duplicate. Statistical analysis was performed using SPSS 19.0 software (SPSS, Chicago, USA). The unpaired Student *t*-test was used to compare group means. Differences were considered significant if P < 0.05.

Results

Effect of pyloric ligation on the expression of serum enzymes and bilirubins

The expression levels of serum AST, ALT, and ALP were significantly increased in the model group than in the control group (P < 0.05 or 0.01). Furthermore, the levels of BILD2 and BILT3 were also significantly higher in the model group than in the control group (P < 0.01) (**Table 1**).

Effect of pyloric ligation on the content of liver GSH-PX and liver index

The GSH-PX in liver was significantly lower in the model rats than in the controls (P < 0.05, 210.76 $U \cdot L^{-1}$ *vs.* 259.12 $U \cdot L^{-1}$). By contrast, the liver index in the in the model rats was significantly higher than in the controls (P < 0.05, 2.88% *vs.* 2.67%) (**Table 2**).

Identified DEPs

Based on the protein spectrum data, using the criterion of 1% FDR, 6095 kinds of proteins and

Table 3. The enriched GO and pathway terms of the differentially expressed proteins

Category	GO ID	Terms	Corrected *P*-value	Protein count	Gene symbols of proteins
BP	GO:1990267	Response to transition metal nanoparticle	0.002272711	9	*Sod3*, *Cyp17a1*, *Tat*, *Mt2A*, *S100a8*, *Hmox1*, *Abat*, *S100a9*, *Mt1*
	GO:0010038	Response to metal ion	0.004125784	13	*Pcsk1*, *Sod3*, *Tat*, *Mt2A*, *Junb*, *S100a8*, *Hsd17b2*, *S100a9*, *Abat*, *Fgb*, *Hmox1*, *Mt1*, *Fgg*
	GO:0006950	Response to stress	0.005367404	40	*Cyp17a1*, *Slc7a2*, *Mgst1*, *S100a8*, *Orm1*, *Slc38a3*, *Serpina3n*, *Ptpn2*, *Hmox1*, *LOC688090*, *Map1lc3b*, *Aldh2*, *Mt2A*, *Abhd2*, *Taok1*, *Pdcd4*, *Mbl2*, *P08932*, *Abat*, *Hpx*, *A2m*, *Morf4l2*, *Ngp*, *Mt1*, *Fgb*, *S100a9*, *Pcsk1*, *Np4*, *Sod3*, *Tat*, *Ifrd1*, *Rnase4*, *Anxa1*, *Fam129a*, *Aldh2*, *Camp*, *Pkm*, *Polr3b*, *Mcam*, *Fgg*
	GO:0010035	Response to inorganic substance	0.005644165	15	*Pcsk1*, *Sod3*, *Sepp1*, *Tat*, *Mt2A*, *Junb*, *S100a8*, *Anxa1*, *Hsd17b2*, *S100a9*, *Abat*, *Fgb*, *Hmox1*, *Mt1*, *Fgg*
	GO:0016485	Protein processing	0.006073176	14	*Pcsk1*, *Mbl2*, *Mcpt10*, *Ngp*, *Sec11c*, *S100a8*, *Serpina3k*, *S100a9*, *Mcpt8l2*, *Camp*, *Serpina3n*, *P08932*, *Spcs3*, *A2m*
	GO:0045087	Innate immune response	0.008010367	12	*Np4*, *Ptpn2*, *Fgb*, *S100a8*, *S100a9*, *Mbl2*, *Camp*, *Serpina3n*, *Hpx*, *A2m*, *Polr3b*, *LOC688090*
	GO:0006067	Ethanol metabolic process	0.012901892	3	*Adh6*, *Aldh2*, *Aldh1A1*
	GO:0032496	Response to lipopolysaccharide	0.012901892	11	*Pcsk1*, *Aldh2*, *Cyp17a1*, *Mgst1*, *S100a8*, *Orm1*, *Aldh2*, *Camp*, *Serpina3n*, *S100a9*, *Bysl*
	GO:0070555	Response to interleukin-1	0.014857327	6	*Pcsk1*, *Anxa1*, *Camp*, *Serpina3n*, *Fgb*, *Bysl*
	GO:0002237	Response to molecule of bacterial origin	0.016682739	11	*Pcsk1*, *Aldh2*, *Cyp17a1*, *Mgst1*, *S100a8*, *Orm1*, *Aldh2*, *Camp*, *Serpina3n*, *S100a9*, *Bysl*
	GO:0009617	Response to bacterium	0.018317417	13	*Pcsk1*, *Np4*, *Aldh2*, *Cyp17a1*, *Mgst1*, *S100a8*, *Orm1*, *Aldh2*, *Mbl2*, *Camp*, *Serpina3n*, *S100a9*, *Bysl*
	GO:0006955	Immune response	0.020150079	17	*Mbl2*, *Np4*, *Fgb*, *Mcpt10*, *Ptpn2*, *C1r*, *S100a8*, *Orm1*, *Hmox1*, *Mcpt8l2*, *Camp*, *Serpina3n*, *Hpx*, *A2m*, *Polr3b*, *S100a9*, *LOC688090*
	GO:0006952	Defense response	0.020150079	18	*Np4*, *Fgb*, *Ptpn2*, *Ngp*, *Slc7a2*, *S100a8*, *Orm1*, *Hmox1*, *Mbl2*, *Camp*, *Serpina3n*, *P08932*, *Hpx*, *A2m*, *Polr3b*, *S100a9*, *LOC688090*, *Fgg*
	GO:0034097	Response to cytokine	0.020150079	13	*Pcsk1*, *Cyp17a1*, *Ptpn2*, *Junb*, *Mt2A*, *Fgb*, *Anxa1*, *Camp*, *Serpina3n*, *Hpx*, *Lifr*, *LOC688090*, *Bysl*
	GO:0006959	Humoral immune response	0.036024283	6	*Np4*, *C1r*, *Camp*, *Mbl2*, *Hpx*, *A2m*
	GO:0033993	Response to lipid	0.043158481	18	*Pcsk1*, *Aldh2*, *Cyp17a1*, *Tat*, *Mgst1*, *Hsd17b2*, *Junb*, *S100a8*, *Orm1*, *Anxa1*, *S100a9*, *P02761*, *Camp*, *Serpina3n*, *A2m*, *Aldh2*, *Hmox1*, *Bysl*
	GO:0009611	Response to wounding	0.043158481	14	*Pcsk1*, *Slc7a2*, *Pkm*, *Fgb*, *S100a8*, *Abhd2*, *Hmox1*, *S100a9*, *Mbl2*, *Ptpn2*, *A2m*, *Mcam*, *Ifrd1*, *Fgg*
	GO:0006954	Inflammatory response	0.045755216	11	*Slc7a2*, *S100a8*, *Orm1*, *Hmox1*, *Mbl2*, *Serpina3n*, *P08932*, *Ptpn2*, *A2m*, *S100a9*, *Fgg*
CC	GO:0005615	Extracellular space	0.000133835	26	*P02761*, *S100a8*, *Orm1*, *Serpina3k*, *Serpina3n*, *Apoc2*, *Mbl2*, *P08932*, *Hpx*, *A2m*, *Ces1c*, *Irf2bpl*, *C1r*, *Igfals*, *Fgb*, *S100a9*, *Pcsk1*, *Np4*, *Sod3*, *Sepp1*, *Inhbe*, *Anxa1*, *Camp*, *Itm2b*, *Mcam*, *Fgg*
	GO:0072562	Blood microparticle	0.005367404	7	*C1r*, *Orm1*, *Fgb*, *Serpina3n*, *Hpx*, *A2m*, *Fgg*
	GO:0044421	Extracellular region part	0.030068326	41	*Adh6*, *P02761*, *S100a8*, *Orm1*, *Serpina3k*, *Serpina3n*, *Apoc2*, *Aldh2*, *Pkm*, *Taok1*, *Vps37b*, *Mbl2*, *P08932*, *Abat*, *Hpx*, *A2m*, *Steap4*, *Ces1c*, *Slc4a4*, *Irf2bpl*, *C1r*, *Igfals*, *Tgm1*, *Fgb*, *S100a9*, *Pcsk1*, *Np4*, *Sod3*, *Esam*, *Sepp1*, *Lifr*, *Rnase4*, *Inhbe*, *Anxa1*, *Fam129a*, *Aldh2*, *Stambp*, *Camp*, *Fgg*, *Mcam*, *Itm2b*
KEGG pathway	rno04610	Complement and coagulation cascades	0.005644	7	*Fga*, *Kng2*, *C1r*, *Fgb*, *Mbl2*, *A2m*, *Fgg*
KEGG pathway	rno05150	Staphylococcus aureus infection	0.033547	5	*Mbl2*, *C1r*, *RT1-Db1a*, *LOC688090*, *Fgg*

GO, Gene Ontology; KEGG, Kyoto Encyclopedia of Genes and Genomes; BP, biological process; CC, cellular component.

47538 kinds of polypeptides were identified and quantified. Following the criteria of FDR < 0.05 and FC > 1.5, a total of 147 DEPs were identified, including 80 upregulated and 67

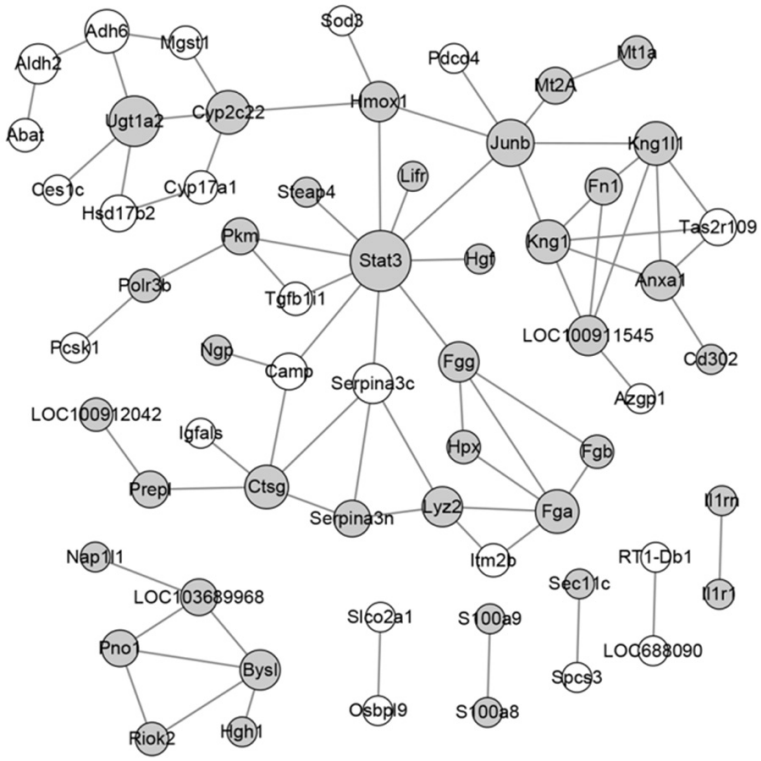

Figure 2. The protein-protein interaction network consisting of differentially expressed proteins. The grey nodes represent the upregulated proteins in liver injury models, and the white nodes represent the downregulated proteins in liver injury models.

downregulated DEPs. The clustering heat map revealed that these DEPs were able to distinguish the model samples from the control samples (**Figure 1**).

Potential functions of the DEPs

To further reveal the potential biological functions of the identified DEPs, the GO and KEGG pathway enrichment analyses were performed. A total of 18 significant GO terms in biological process (BP) and 3 terms in cellular component (CC) were enriched by the DEPs. For example, *Hmox1* and *Fgg* were involved in GO terms like "defense response" and "inflammatory response"; *Junb* was related to "response to cytokine" (**Table 3**).

Analysis of the PPI network

To further investigate the interactions of the DEPs, a PPI network was constructed. The PPI network consisted of 63 proteins and 73 PPI pairs. In this network, upregulated *Stat3* had the highest degree, and it interacted with 10 proteins, such as upregulated *Junb* and *Hmox1*, as well as downregulated *Serpina3c* and *Tgfb1i1* (**Figure 2**).

Furthermore, the potential functions of proteins in the PPI network were explored. A series of significant GO terms were enriched by the proteins in the network. For instance, *Stat3* and *Hmox1* were enriched in the GO terms about immunity, such as "defense response", "inflammatory response", and "response to cytokine stimulus" (**Table 4**). Meanwhile, 9 significant KEGG pathways were enriched by the proteins, such as "complement and coagulation cascades" (e.g. *Fgg*, *Fga*, *Fgb*), and "steroid hormone biosynthesis" (e.g. *Ugt1a2*) (**Table 5**).

Discussion

In the present study, the rat liver injury models were established by pyloric ligation. The liver index and the expression levels of serum AST, ALT and ALP, as well as BILD2 and BILT3, were significantly higher in the model group than in the control group. By contrast, liver GSH-PX was significantly lower in the model rats than in the controls. These results indicated that the rat liver injury models were successfully established. Furthermore, the liver protein spectrum was analyzed using HPLC-MS. A total of 147 DEPs were identified, including 80 upregulated and 67 downregulated DEPs. In the PPI network, upregulated *Stat3* had the highest degree, and it interacted with upregulated proteins such as *Junb*, *Fgg*, and *Hmox1*, as well as downregulated *Serpina3c* and *Tgfb1i1*.

Stat3 encodes signal transducer and activator of transcription 3, which is activated by tyrosine phosphorylation during the response to interleukin-6 (IL-6) and epidermal growth factor [10]. In this study, *Stat3* was predicted to be associated with immunity. In the liver acute phase response, *STAT3* plays a key role along with IL-6 [11]. Multiple previous studies have found that *STAT3* is associated with liver injury. For instance, *Stat3* signaling activation cross-linking transforming growth factor-β1 in hepatic stellate cell contributes to the exacerbation of liver injury and fibrosis [12]. IL-6/*STAT3* signal-

Table 4. The top 10 enriched GO terms in each category by the proteins in the PPI network

Category	Term	Gene count	*P*-value	Gene symbols of proteins
BP	GO: 0006952~defense response	13	7.00E-08	*Kng1*, *Lyz2*, *Il1R1*, *S100A8*, *Camp*, *Kng1L1*, *Il1Rn*, *Stat3*, *Serpina3N*, *Fgg*, *Hmox1*, *Np4*, *Fn1*
BP	GO: 0009611~response to wounding	12	1.16E-06	*Kng1*, *Pcsk1*, *Fgg*, *Serpina3N*, *Fga*, *S100A8*, *Fgb*, *Hmox1*, *Il1Rn*, *Kng1L1*, *Stat3*, *Fn1*
BP	GO: 0010035~response to inorganic substance	10	1.52E-06	*Pcsk1*, *Fgg*, *Fga*, *Mt1A*, *Fgb*, *Hmox1*, *Mt2A*, *Anxa1*, *Abat*, *Sod3*
BP	GO: 0006954~inflammatory response	9	3.10E-06	*Kng1*, *Fgg*, *Serpina3N*, *S100A8*, *Hmox1*, *Il1Rn*, *Kng1L1*, *Stat3*, *Fn1*
BP	GO: 0034097~response to cytokine stimulus	7	7.08E-06	*Pcsk1*, *Il1R1*, *Serpina3N*, *Anxa1*, *Lifr*, *Junb*, *Stat3*
BP	GO: 0010038~response to metal ion	8	8.60E-06	*Pcsk1*, *Fgg*, *Fga*, *Mt1A*, *Fgb*, *Mt2A*, *Abat*, *Sod3*
BP	GO: 0006953~acute-phase response	5	1.05E-05	*Kng1*, *Il1Rn*, *Kng1L1*, *Stat3*, *Fn1*
BP	GO: 0014070~response to organic cyclic substance	8	2.69E-05	*Pcsk1*, *Hmox1*, *Il1Rn*, *Aldh2*, *Anxa1*, *Abat*, *Junb*, *Stat3*
BP	GO: 0048545~response to steroid hormone stimulus	8	2.03E-04	*Pcsk1*, *Ugt1A2*, *Hmox1*, *Il1Rn*, *Aldh2*, *Anxa1*, *Junb*, *Stat3*
BP	GO: 0009617~response to bacterium	7	2.52E-04	*Pcsk1*, *Lyz2*, *Camp*, *Il1Rn*, *Np4*, *Aldh2*, *Mgst1*
CC	GO: 0005615~extracellular space	14	6.10E-08	*Kng1*, *Il1Rn*, *Kng1L1*, *Anxa1*, *Igfals*, *Hgf*, *Sod3*, *Pcsk1*, *Azgp1*, *Fgg*, *Fga*, *Fgb*, *Np4*, *Fn1*
CC	GO: 0005577~fibrinogen complex	4	2.71E-07	*Fgg*, *Fga*, *Fgb*, *Fn1*
CC	GO: 0044421~extracellular region part	14	3.08E-06	*Kng1*, *Il1Rn*, *Kng1L1*, *Anxa1*, *Igfals*, *Hgf*, *Sod3*, *Pcsk1*, *Azgp1*, *Fgg*, *Fga*, *Fgb*, *Np4*, *Fn1*
CC	GO: 0030141~secretory granule	8	2.06E-05	*Pcsk1*, *Fgg*, *Lyz2*, *Fga*, *Fgb*, *Camp*, *Hgf*, *Fn1*
CC	GO: 0031093~platelet alpha granule lumen	5	2.17E-05	*Fgg*, *Fga*, *Fgb*, *Hgf*, *Fn1*
CC	GO: 0060205~cytoplasmic membrane-bounded vesicle lumen	5	2.91E-05	*Fgg*, *Fga*, *Fgb*, *Hgf*, *Fn1*
CC	GO: 0005576~extracellular region	17	3.22E-05	*Kng1*, *Camp*, *Il1Rn*, *Kng1L1*, *Anxa1*, *Igfals*, *Hgf*, *Sod3*, *Azgp1*, *Pcsk1*, *Serpina3N*, *Fgg*, *Fga*, *Hpx*, *Fgb*, *Np4*, *Fn1*
CC	GO: 0031983~vesicle lumen	5	4.52E-05	*Fgg*, *Fga*, *Fgb*, *Hgf*, *Fn1*
CC	GO: 0031091~platelet alpha granule	5	6.69E-05	*Fgg*, *Fga*, *Fgb*, *Hgf*, *Fn1*
CC	GO: 0031982~vesicle	11	2.18E-04	*Pcsk1*, *Fgg*, *Lyz2*, *Fga*, *Ngp*, *Fgb*, *Camp*, *Il1Rn*, *Nap1L1*, *Hgf*, *Fn1*
MF	GO: 0030674~protein binding, bridging	4	5.91E-04	*Fgg*, *Fga*, *Fgb*, *Anxa1*
MF	GO: 0043499~eukaryotic cell surface binding	3	1.74E-03	*Fgg*, *Fga*, *Fgb*
MF	GO: 0043498~cell surface binding	3	5.04E-03	*Fgg*, *Fga*, *Fgb*
MF	GO: 0008236~serine-type peptidase activity	5	6.54E-03	*Pcsk1*, *Sec11C*, *Prepl*, *Hgf*, *Ctsg*
MF	GO: 0017171~serine hydrolase activity	5	6.65E-03	*Pcsk1*, *Sec11C*, *Prepl*, *Hgf*, *Ctsg*
MF	GO: 0005506~iron ion binding	5	2.12E-02	*Steap4*, *Cyp17A1*, *Hpx*, *Hmox1*, *Cyp2C22*
MF	GO: 0005507~copper ion binding	3	2.24E-02	*Steap4*, *Mt1A*, *Sod3*
MF	GO: 0004252~serine-type endopeptidase activity	4	2.55E-02	*Pcsk1*, *Prepl*, *Hgf*, *Ctsg*
MF	GO: 0019838~growth factor binding	3	4.23E-02	*Il1R1*, *Lifr*, *Igfals*
MF	GO: 0046872~metal ion binding	17	4.25E-02	*Steap4*, *S100A8*, *S100A9*, *Anxa1*, *Adh6*, *Stat3*, *Sod3*, *Pcsk1*, *Cyp17A1*, *Fgg*, *Mt1A*, *Hpx*, *Hmox1*, *Mt2A*, *Tgfb1I1*, *Fn1*, *Cyp2C22*

GO, Gene Ontology; BP, biological process; CC, cellular component; MF, molecular function; PPI, protein-protein interaction.

ing promoted by placental stem cells induces the proliferation of hepatic cells in a carbon tetrachloride-injured liver rat model [13]. Moreover, *STAT3* activation promotes the protective effect of IL-11 treatment on the liver ischemia/reperfusion injury [14]. A recent study has reported that *STAT3* signaling is correlated with the protective effect of chlorogenic acid on cholestatic liver injury in mice [15]. These results indicate that *Stat3* has a potential role in the liver injury likely through various cytokines.

In this study, upregulated proteins such as *Junb*, *Fgg* and *Hmox1* were predicted to interact with *Stat3*. *Junb* (Jun B Proto-Oncogene) is involved in multiple cell processes, such as cell proliferation, differentiation and invasion [16, 17]. In the liver injury mice, *Junb* expression is altered during the liver regeneration [18]. A previous study has discovered that *JUNB* is specifically expressed in human and murine immunocytes during acute liver injury, and it mediates the expression of interferon-γ [19]. *Hmox1* interacted with both *Stat3* and *Junb* in the cur-

Table 5. The enriched significant KEGG pathways by the proteins in the PPI network

Term	Gene count	*P*-value	Gene symbols of proteins
rno00980: Metabolism of xenobiotics by cytochrome P450	4	1.57E-03	*Ugt1A2*, *Adh6*, *Mgst1*, *Cyp2C22*
rno04610: Complement and coagulation cascades	4	2.44E-03	*Kng1*, *Fgg*, *Fga*, *Fgb*
rno00982: Drug metabolism	4	2.65E-03	*Ugt1A2*, *Adh6*, *Mgst1*, *Cyp2C22*
rno00140: Steroid hormone biosynthesis	3	1.21E-02	*Cyp17A1*, *Hsd17B2*, *Ugt1A2*
rno00830: Retinol metabolism	3	2.21E-02	*Ugt1A2*, *Adh6*, *Cyp2C22*
rno05322: Systemic lupus erythematosus	3	4.81E-02	*Rt1-Db1*, *Ctsg*, *Loc688090*

KEGG, Kyoto Encyclopedia of Genes and Genomes; PPI, protein-protein interaction.

rent study. During liver regeneration after liver injury in mice, *Hmox1* is highly expressed [20, 21]. *Fgg* encodes the gamma component of fibrinogen, which has a major function in hemostasis as one of the primary components of blood clots [22]. *Fgg* has been found to be highly expressed in liver-injured mice, compared with the controls [15]. These results suggest that *Junb*, *Fgg,* and *Hmox1* may also play critical roles in the liver injury likely via the interactions with *Stat3*.

Furthermore, several downregulated proteins were predicted to interact with *Stat3*, such as *Serpina3c* and *Tgfb1i1*. *Serpina3c* protein is a serine protease inhibitor [23]. Previous studies have reported that *Serpina3c* takes part in the immune system [24, 25]. *Tgfb1i1* (transforming growth factor beta 1 induced transcript 1), also known as *HIC5*, is a coactivator of the androgen receptor [26]. A recent study has demonstrated that deficiency of Hic-5 weakens the activation of mice hepatic stellate cells and liver fibrosis via the upregulation of Smad7 [27]. There is no other study to support the associations of *Serpina3c* and *Tgfb1i1* with liver injury. We speculated that these two proteins might participate in liver injury via immunity or the interaction with *Stat3*.

Despite the aforementioned results, there were several limitations in this study. The predictions needed to be confirmed by experiments. In our further study, the expressions of the proteins (e.g. *Stat3*, *Junb*, *Fgg*, *Hmox1*, *Serpina3c* and *Tgfb1i1*), and their interactions in injured liver will be confirmed by experiments.

In conclusion, based on the protein spectrum data from HPLC-MS, 80 upregulated and 67 downregulated DEPs were identified in the established rat liver injury model. The immunity-related *Stat3* and some proteins (e.g. *Junb*, *Fgg*, *Hmox1*, *Serpina3c* and *Tgfb1i1*) interacting with it may be likely associated with liver injury. These results will be further verified and are expected to provide novel information for the diagnosis and therapy of liver injury.

Acknowledgements

This study was supported by the National Natural Science Foundation of China (No. 814-41105 and No. 81360673), Inner Mongolia Autonomous Region Science and Technology Major Project (No. GCY20150833) and Doctoral Startup Fund of Inner Mongolia National University (No. BS413).

Disclosure of conflict of interest

None.

Address correspondence to: Bagenna Bao, School of Mongolian Medicine and Pharmaceutical Sciences, Inner Mongolia University for The Nationalities, 996, Xi La Mu Lun Road, Horqin District, Tongliao 028000, Inner Mongolia, P. R. China. Tel: +86-475-8314242; Fax: +86-475-8314242; E-mail: baobagenna68@hotmail.com; Tuul Khalzaabaast, College of Mongolian Medicine, Inner Mongolia University for The Nationalities, 996, Xi La Mu Lun Road, Horqin District, Tongliao 028000, Inner Mongolia, P. R. China. Tel: +86-475-8314242; Fax: +86-475-8314242; E-mail: 2217533243@qq.com

References

[1] AR, Koch DG and Lee WM. Drug-induced acute liver failure: results of a U.S. multicenter, prospective study † ‡ §. Hepatology 2010; 52: 2065-2076.

[2] Kaplowitz N. Drug-induced liver injury. Drug Safety An International Journal of Medical Toxicology & Drug Experience 2007; 30: 277-294.

[3] Bell LN, Vuppalanchi R, Watkins PB, Bonkovsky HL, Serrano J, Fontana RJ, Wang M, Rochon J and Chalasani N. Serum proteomic profiling in patients with drug-induced liver injury. Aliment Pharmacol Ther 2012; 35: 600-612.

[4] Matsuo Y, Irie K, Kiyonari H, Okuyama H, Nakamura H, Son A, Lopez-Ramos DA, Tian H, Oka S

and Okawa K. The protective role of the transmembrane thioredoxin-related protein TMX in inflammatory liver injury. Antioxid Redox Signal 2013; 18: 1263-1272.
[5] Brenner DA. Fra, Fra away: the complex role of activator protein 1 in liver injury. Hepatology 2014; 59: 19-20.
[6] Buck M, Solis-Herruzo J and Chojkier M. C/EBPβ-Thr217 phosphorylation stimulates macrophage inflammasome activation and liver Injury. Sci Rep 2016; 6: 24268.
[7] Xie C, Mao X, Huang J, Ding Y, Wu J, Dong S, Kong L, Gao G, Li CY and Wei L. KOBAS 2.0: a web server for annotation and identification of enriched pathways and diseases. Nucleic Acids Res 2011; 39: 316-322.
[8] Szklarczyk D, Franceschini A, Wyder S, Forslund K, Heller D, Huerta-Cepas J, Simonovic M, Roth A, Santos A, Tsafou KP, Kuhn M, Bork P, Jensen LJ and von Mering C. STRING v10: protein-protein interaction networks, integrated over the tree of life. Nucleic Acids Res 2015; 43: D447-452.
[9] Kohl M, Wiese S and Warscheid B. Cytoscape: software for visualization and analysis of biological networks. Methods Mol Biol 2011; 696: 291-303.
[10] Zhong Z, Wen Z and Jr DJ. Stat3: a STAT family member activated by tyrosine phosphorylation in response to epidermal growth factor and interleukin-6. Science 1994; 264: 95-98.
[11] He G and Karin M. NF-κB and STAT3 - key players in liver inflammation and cancer. Cell Research 2011; 21: 159-168.
[12] Xu MY, Hu JJ, Shen J, Wang ML, Zhang QQ, Qu Y and Lu LG. Stat3 signaling activation crosslinking of TGF-β1 in hepatic stellate cell exacerbates liver injury and fibrosis. Biochimica Et Biophysica Acta 2014; 1842: 2237–2245.
[13] Jung J, Ji WM, Choi JH, Yong WL, Park SH and Kim GJ. Epigenetic alterations of IL-6/STAT3 signaling by placental stem cells promote hepatic regeneration in a rat model with CCl4-induced liver injury. Int J Stem Cells 2015; 8: 79-89.
[14] Zhu M, Lu B, Cao Q, Wu Z, Xu Z, Li W, Yao X and Liu F. IL-11 attenuates liver ischemia/reperfusion injury (IRI) through STAT3 signaling pathway in mice. PLoS One 2015; 10: e0126296.
[15] Tan Z, Luo M, Yang J, Cheng Y, Huang J, Lu C, Song D, Ye M, Dai M, Gonzalez FJ, Liu A, Guo B. Chlorogenic acid inhibits cholestatic liver injury induced by α-naphthylisothiocyanate: involvement of STAT3 and NFκB signalling regulation. J Pharm Pharmacol 2016; 68: 1203-1213.
[16] Piechaczyk M and Farràs R. Regulation and function of JunB in cell proliferation. Biochem Soc Trans 2008; 36: 864-867.
[17] Kanno T, Kamba T, Yamasaki T, Shibasaki N, Saito R, Terada N, Toda Y, Mikami Y, Inoue T and Kanematsu A. JunB promotes cell invasion and angiogenesis in VHL-defective renal cell carcinoma. Oncogene 2012; 31: 3098-3110.
[18] Nakamura K, Nonaka H, Saito H, Tanaka M and † AM. Hepatocyte proliferation and tissue remodeling is impaired after liver injury in oncostatin M receptor knockout mice. Hepatology 2004; 39: 635-644.
[19] Thomsen MK, Bakiri L, Hasenfuss SC, Hamacher R, Martinez L, Wagner EF. JUNB/AP-1 controls IFN-γ during inflammatory liver disease. J Clin Invest 2013; 123: 5258-5268.
[20] Cho KA, Woo SY, Seoh JY, Han HS and Ryu KH. Mesenchymal stem cells restore CCl 4 -induced liver injury by an antioxidative process. Cell Biol Int 2012; 36: 1267-1274.
[21] Su AI, Guidotti LG, Pezacki JP, Chisari FV and Schultz PG. Gene expression during the priming phase of liver regeneration after partial hepatectomy in mice. Proc Natl Acad Sci U S A 2002; 99: 11181-11186.
[22] Wu C and Chung AE. Potential role of entactin in hemostasis. Specific interaction of entactin with fibrinogen A alpha and B beta chains. J Biol Chem 1991; 266: 18802-18807.
[23] Heit C, Jackson BC, Mcandrews M, Wright MW, Thompson DC, Silverman GA, Nebert DW and Vasiliou V. Update of the human and mouse SERPIN gene superfamily. Hum Genomics 2012; 7: 5241-5252.
[24] Onaivi ES, Schanz N and Lin ZC. Psychiatric disturbances regulate the innate immune system in CSF of conscious mice. Transl Psychiatry 2014; 4: e367.
[25] Cannella AP, Tsolis RM, Li L, Felgner PL, Saito M, Sette A, Gotuzzo E and Vinetz JM. Antigen-specific acquired immunity in human brucellosis: implications for diagnosis, prognosis, and vaccine development. Front Cell Infect Microbiol 2012; 2: 1.
[26] Fujimoto N, Yeh S, Kang HY, Inui S, Chang HC, Mizokami A and Chang C. Cloning and characterization of androgen receptor coactivator, ARA55, in human prostate. J Biol Chem 1999; 274: 8316-8321.
[27] Lei XF, Fu W, Kim-Kaneyama JR, Omoto T, Miyazaki T, Li B and Miyazaki A. Hic-5 deficiency attenuates the activation of hepatic stellate cells and liver fibrosis through upregulation of Smad7 in mice. J Hepatol 2016; 64: 110-117.